Available online at www.sciencedirect.com
SCIENCE DIRECT®
Journal of Nuclear Materials 337–339 (2005) 654–658
journal of nuclear materials
www.elsevier.com/locate/jnucmat

Hydrogen release behavior from graphite under pulsed laser irradiation

T. Shibahara *, Y. Sakawa, T. Tanabe

Department of Nuclear Engineering, Graduate School of Engineering, Nagoya University, Furo-cho, Chikusa-ku, Nagoya 464-8603, Japan

Abstract

Mass distribution and time variation of the emitted ions by time-of-flight mass spectrometer and desorbed gases by a quadrupole mass spectrometer from the H^+-implanted graphite sample by the pulsed ArF (193 nm) laser irradiation have been studied. The averaged ion mass is smaller for the larger laser fluence. Most of the implanted H in the laser irradiated area was released out after a few 10 shots, when the laser fluence is above the ablation threshold. However, the ablation accompanies large amount of hydrocarbon release. Changing the power of the laser, the reduction of hydrocarbon release is studied.

PACS: 79.20.D; 79.20.L; 33.80.G; 28.52; 81.05.T
Keywords: Laser ablation; Laser application; Graphite; Tritium retention; Tritium removal

1. Introduction

In D–T fusion devices, carbon materials used as plasma facing materials retain large amount of tritium. From safety concern, tritium remaining in the devices has to be removed periodically. Therefore, the development of the tritium removal method is one of the key issues for ITER [1]. One of the methods to remove tritium is baking. If carbon materials are baked over 1000 K, most of tritium accumulated near surface region can be removed [2,3]. However, it is technically difficult to heat up a whole tokamak device. Recently, a laser induced desorption (LID) technique has been proposed as one of the tritium removal methods. The LID technique has following advantages: Laser beam can be introduced into any places thorough fibers and optics, and can give very high power density by beam focusing. Skinner et al. [4] have used a CW laser beam as a heat source for the tritium removal from codeposits on carbon tiles. Additionally, if the laser power is sufficiently large, surface components are removed drastically by laser ablation. Shu et al. have used ArF pulsed laser devices in the ablative conditions to remove hydrogen from the codeposits on carbon tiles [5].

In order to optimize the LID method for hydrogen release, chemical species released by the laser irradiation have to be examined. By the laser irradiation, many chemical species desorb, including various hydrocarbons, carbon clusters, hydrogen molecules, and other molecules. However, most of hydrocarbons have large sticking coefficients to easily stick near laser irradiated area [6,7], desorb again and contaminate the inside of the vacuum vessel resulting in harmful effects on the

* Corresponding author.
E-mail address: h022402d@mbox.nagoya-u.ac.jp (T. Shibahara).

0022-3115/$ - see front matter © 2004 Elsevier B.V. All rights reserved.
doi:10.1016/j.jnucmat.2004.10.154

tritium removal system. Since tritiated hydrocarbons are more hazardous than tritium gas, it is seems to be more suitable that accumulated tritium is removed as tritium gas.

In this paper, we present experimental investigations of the hydrogen release behavior by irradiating ArF excimer laser on the graphite target in which 10 keV H^+ ions were implanted. By varying the laser fluence, we compare the hydrogen release behavior both in ablation and non-ablation conditions.

2. Experimental

Experiments were conducted in an ultra-high vacuum chamber ($<4\times10^{-6}$ Pa) equipped with a quadrupole mass spectrometer (QMS) and a time-of-flight mass spectrometer (TOFMS). We used the IG-110U graphite plate (Toyo Tanso Ltd.) as a sample. H^+ ion beams were produced by an ion gun with the energy of 10 keV, and implanted to the sample from the normal to the surface plane with the beam size of 8 mm in diameter. By using Transport of Ions in Matter (TRIM) code, for the implanted 10 keV H^+ ions with the fluence of 1×10^{22} ions/m^2, it is estimated that the ions exist 250 nm range from the surface and that the H/C ratio on the implanted area is ~0.45. The value is similar to the H/C (0.4) of hydrogen codeposited carbon film observed in carbon wall tokamaks. After the H^+ implantation, a pulsed ArF laser beam (wave length: 193 nm, energy: 5–10 mJ/pulse, pulse width: ~8 ns and Rep. rate: 5 Hz) was irradiated to the sample. The laser beam was focused on the sample surface by a quartz lens of the focal length of 300 mm through a sapphire window and irradiated from 45° to the normal plane. We varied the laser fluence (F = 0.3–11.8 J/cm^2) by changing both the laser pulse energy and the distance between the lens and the sample.

In TOFMS, emitted ions were accelerated by the electrical field of a drift-tube and detected by a micro-channel plate (MCP). The length of the drift tube is long enough to completely separate all emitted ions if their initial velocities are nearly zero. Hence the overlap of TOFMS spectra observed in the present experiments can be attributed not only the overlap of neighboring masses but also the difference or wide distribution of initial velocities of the emitted ions.

We have determined amounts of desorbed gases from their partial pressure increase in the target chamber measured by QMS (0.6–0.84 s/scan, scan range is m/e = 1–80) and an ionization gauge. Since the gas desorption rate by the laser irradiation was larger than the pumping speed of this system, we could measure desorbed gas molecules using QMS. We have measured the desorbed ions and gases during the 2000 shots of laser irradiation.

3. Results and discussions

Fig. 1 shows the mass distributions of the emitted ions at the second and the 50th laser shots measured by TOFMS for the samples with and without H^+ implantation under the laser fluence of F = 11.8 and 0.3 J/cm^2. For F = 11.8 J/cm^2 which is ablation condition, the signal intensities of TOFMS were more than an order of magnitude larger than that for F = 0.3 J/cm^2 (no-ablation), while the averaged mass number of the released ions was smaller. For the H^+ implanted sample, both TOFMS signal intensities and the released ion mass were larger than those for the un-implanted sample and decreased with increasing the shot number. The ionization energy (IE) of C atom is11.26 eV and those of large-size carbon clusters (C_n, $n \geqslant 6$) are below 10 eV and decrease more with increasing the cluster size [8–11]. For the carbon clusters C_n with $n \geqslant 100$, IEs are between 6.2 and 6.45 eV [11]. Therefore, the ArF laser photons (6.4 eV) could produce larger size carbon cluster ions by one-photon ionization.

Fig. 2 displays changes of the averaged ion mass number $\bar{m}$ (a) and the integrated TOFMS intensities I_{TOFMS} over mass number m/e of 1–200 (b) with the number of the laser shot. In all cases, $\bar{m}$ is above several tens of mass. $\bar{m}$ decreased with the number of the laser shots for all cases as described above. When F = 11.8 J/cm^2, both I_{TOFMS} and $\bar{m}$ for the H^+ implanted sample were larger than those for the un-implanted sample during the initial several laser shots. With increasing the laser shots number, both $\bar{m}$ and I_{TOFMS} decreased, and after about ten laser shots, $\bar{m}$ and I_{TOFMS} for the H^+ implanted sample decreased to nearly the identical levels of the un-implanted sample. Probably most of the implanted H in the laser irradiated area was released out after a few 10 shots under this condition as discussed below. For F = 0.3 J/cm^2, both $\bar{m}$ and I_{TOFMS} for the H^+ implanted sample were also larger than the those of the

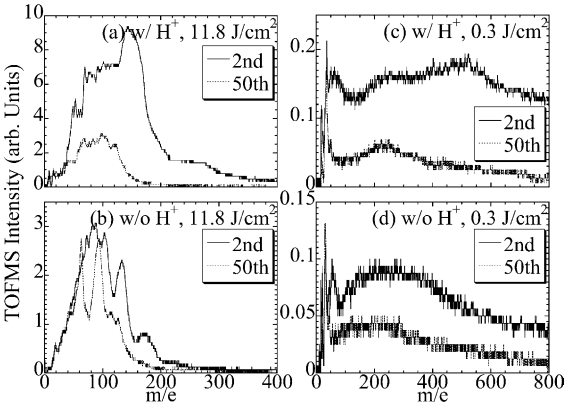

Fig. 1. Mass distributions of the emitted ions measured by TOFMS at the second and the 50th shots.

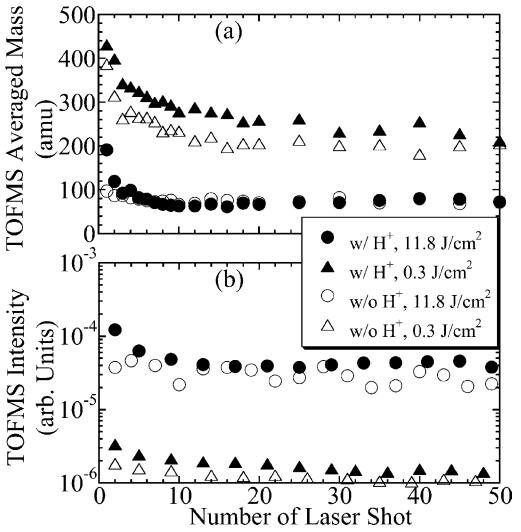

Fig. 2. (a) TOFMS averaged ion mass $\bar{m}$ and (b) TOFMS signal intensity I_{TOFMS} integrated over m/e = 1–200 versus the number of the laser shot for the H^+ implanted and un-implanted samples at F = 11.8 and 0.3 J/cm^2.

un-implanted sample, but the difference between two samples was kept over 50 shots. We have found that $\bar{m}$ of the H^+ implanted sample was by a factor of 1.5 larger than that of the un-implanted sample even at the 1000th shot for F = 0.3 J/cm^2. After nearly 2000 shots, most of the hydrocarbon ions disappeared and only C_1^+ and C_3^+ ions remained for F = 11.8 J/cm^2.

Fig. 3 shows time evolutions of QMS signals for dominant masses for the H^+ implanted sample (a) and the un-implanted one (b) with F = 11.8 J/cm^2. At the highest fluences, the gas was released by ablation but not desorption. However in the following, we use the expression of 'desorbed gas' whether desorption process is dominant or not. Before the laser irradiation, QMS signals were dominated by residual gases, mostly m/e = 18 (H_2O), 17 (OH), 2 (H_2), and 44 (CO_2) and their signal intensities stayed constant. By the laser irradiation, the increase of the residual gas species of CO, CO_2 and H_2O was appreciable after subtracting such background. The increase was attributed to repetitive absorption and desorption of residual gases during the laser-off and desorption during the laser-on, and the effect of the residual gas species was not taken into account hereafter. When F = 11.8 J/cm^2, the dominant QMS mass numbers desorbed by the laser irradiation from the H^+ implanted sample were m/e = 2 (H_2), 26 (C_2H_2), and 28 (segment of C_2H_6). The QMS signal intensity of H_2 and hydrocarbon decreased with increasing the laser shot number and became steady state within 30 shots. For the un-implanted sample, the dominant gases released were similar to those before the laser irradiation, and the increases of the QMS signal intensities by the laser irradiation were very small; more than an order of magnitude smaller than those for the H^+ implanted samples. Although the release of H_2 gas was initially observed, its intensity decreased below the noise level within a few shots. For lower fluence (F = 0.3 J/cm^2) laser irradiations, although gas desorption for the implanted sample was slightly larger than the un-implanted sample, the mass distribution of the desorbed gas species was nearly the same as seen in Fig. 3(b) both for the H^+ implanted and un-implanted samples.

Fig. 4 shows changes of TOFMS H^+ signal (a) and QMS H_2 signal (b) with increasing the number of the laser shot for the samples with and without the H^+ implantation for F = 11.8 and 0.3 J/cm^2. When F = 11.8 J/cm^2, the signal intensities of H^+ and H_2 were appreciable for the initial 30 shots for the H^+ implanted

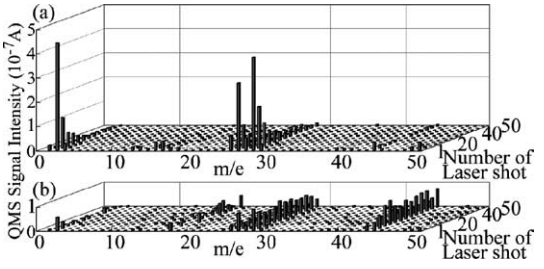

Fig. 3. Time evolution of the mass distributions of the desorbed gases measured by QMS at F = 11.8 J/cm^2. (a) H^+ ions implanted sample and (b) un-implanted sample.

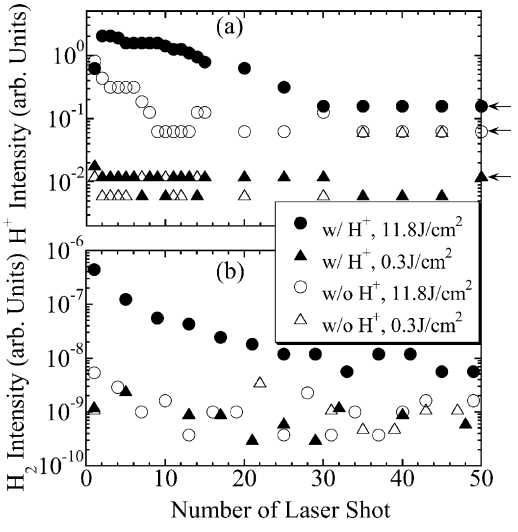

Fig. 4. (a) TOFMS H^+ signal and (b) QMS H_2 signal versus the number of the laser shot for the H^+ implanted and un-implanted samples at F = 11.8 and 0.3 J/cm^2. Horizontal arrows in (a) are the noise level determined by the AD converter.

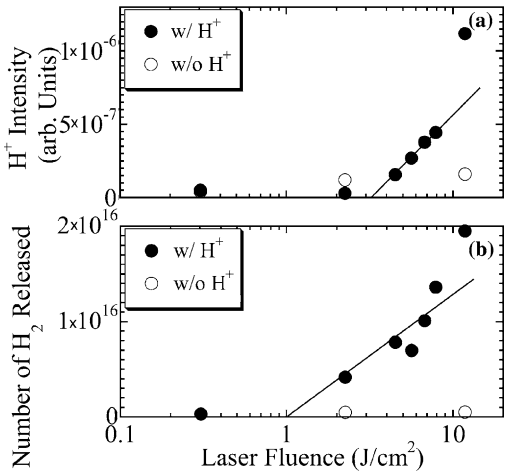

Fig. 5. (a) TOFMS H^+ signal and (b) QMS H_2 signal versus laser fluence for the samples with (●) and without (○) H^+ implantation.

sample, while for the un-implanted sample the H^+ intensity decreased much faster than that for the H^+ implanted sample to be the noise level within 10 shots. H^+ and H_2 signals were remained the noise level for the un-implanted sample, even when $F = 11.8$ J/cm^2.

Fig. 5 shows changes of the integrated intensities of TOFMS H^+ and QMS H_2 signals over the first laser shot to the 50th one with laser fluence. By extrapolation, one can note different thresholds for the H_2 desorption (QMS) and the H^+ emission (TOFMS) at around 1 and 3 J/cm^2, respectively. The former is nearly the same as the measured carbon ablation threshold of 1 J/cm^2 for the ArF laser [5,12], while the latter is a little higher. The lower threshold for H_2 desorption suggests thermal enhancement for H_2 release as discussed below.

Above the ablation threshold, C–H bond breaking occurs rapidly by the ablative phenomena, and thus H^+ and H_2 could be released simultaneously together with various hydrocarbons. Since the bonding energy of C–C bond in graphite is 6.3 eV, the ArF laser photon (193 nm, 6.4 eV) can break the C–C bond. Furthermore, Claeyssens et al. have shown that in a carbon ablation using the ArF laser, a strong one-photon resonance-excitation of the $^1P^0$ state (7.68 eV) occurs from the lowest level of the metastable state (1.26 eV) in an atomic carbon, followed by one-photon ionization of C^+ (ionization energy is 11.26 eV) from the $^1P^0$ state, in other words, resonance-enhanced two-photon ionization could occur [13]. However, in our experiments, we could not clarify the contribution of the resonant bond breaking and/or resonance-enhanced ionization.

Lade and Ashfold have conducted high laser power irradiation ($F \approx 75$ J/cm^2) and observed ablation plume using 193 nm laser irradiation on graphite. They have found that main light emission was from C, C^+ and C_2^+ [14]. In other word, most of ablated materials were fragmented into atom clusters or atoms. We believe that, in our experiment, ablation occurs incompletely even at 11.8 J/cm^2. Actually, for $F = 11.8$ J/cm^2, we observed only C_2 Swan band ($d^3\Pi_g$–$a^3\Pi_u$) emissions, for example at 469.7, 516.5, and 589.9 nm, but not C, C^+ and C_2^+. As seen in the TOFMS spectra, the averaged ion mass was around 60–70 corresponding C_5–C_6 cluster ions. With decreasing the laser fluence, the averaged ion mass or mass number of observed ions in TOFMS increased. This indicates that higher the laser power, smaller the size of the emitted ion clusters (or mass number) owing to the fragmentation in the ablated plume (plasma).

Below the ablation threshold, the laser irradiation results in bulk heating of the target. Accordingly only thermal desorption is possible except some resonant desorption of surface ad- or absorbed molecules. Therefore, most of the hydrogen implanted was retained in the sample.

From these results, it turns out that implanted hydrogen can be removed easily by the ablative laser irradiation. However, in the present laser irradiation condition, the amount of hydrogen released as hydrocarbons was much larger than that of hydrogen molecules, though the hydrocarbon release could be reduced by the high-power fragmentation if the high fluence laser is employed. Nevertheless, carbon atoms and clusters must immediately stick to the vacuum wall, when they impinge, resulting in unwanted contamination of the vacuum wall and also makes quantitative estimation very difficult. Below the ablation threshold, hydrogen molecules and stable hydrocarbons can be released thermally. In order to avoid the release of hydrocarbons, temperature should be raised above 1300 K or more, but above 3000 K carbon clusters like C_2, C_3, C_6 etc. starts to evaporate. In this respect, utilization of CW lasers could be optimized for hydrogen only release. Still one should be very careful for the emission of hydrocarbons and carbon clusters.

4. Conclusions

We have studied mass distribution and time variation of the emitted ions by TOFMS and desorbed gases by QMS from the H^+ implanted graphite sample by the pulsed ArF laser irradiation. Different thresholds for H_2 desorption and H^+ emission are observed at the laser fluence around 1 and 3 J/cm^2, respectively; the former might correspond to the ablation threshold of graphite. In TOFMS measurements, both the averaged ion mass and signal intensity decrease with the number of the laser shot. The averaged ion mass is smaller for the larger laser fluence.

Above the ablation fluence irradiation, most of the implanted hydrogen in the laser irradiated area is

probably released out within several shots, and the averaged ion mass decreases to similar level to that observed for the un-irradiated sample within 10–30 shots. Accordingly, H_2, CH_4 C_2H_2, and C_2H_6, which are dominant in desorbed molecules from the H^+ implanted sample above the ablation threshold, mostly disappear within 30 shots. The released amount of hydrogen is dominated by hydrocarbons, and contribution of H_2 molecules is very small.

Below the ablation threshold, hydrogen is mostly released as H_2 molecules, however, the release is more than one order of magnitude smaller than that observed just above the ablation threshold. In order to achieve effective removal of hydrogen below the ablation threshold, where laser heating is the dominant hydrogen-release mechanism, it might be better to use longer pulse width as described in Ref. [4].

References

[1] G. Federici et al., J. Nucl. Mater. 266–269 (1999) 14.
[2] R.A. Causey et al., J. Nucl. Mater. 176&177 (1990) 987.
[3] T. Tanabe et al., J. Nucl. Mater. 313–316 (2003) 478.
[4] C.H. Skinner et al., J. Nucl. Mater. 301 (2002) 98.
[5] W.M. Shu et al., J. Nucl. Mater. 313–316 (2003) 584.
[6] A. von Keudell et al., Nucl. Fus. 39 (1999) 1451.
[7] W. Jacob, these Proceedings. doi:10.1016/j.jnucmat.2004.10.035.
[8] Y. Kato et al., Chem. Phys. Lett. 386 (2004) 279.
[9] R. Ramanathan et al., J. Chem. Phys. 98 (1993) 7838.
[10] S.B.H. Bach et al., J. Chem. Phys. 98 (1990) 358.
[11] J.A. Zimmerman et al., J. Chem. Phys. 94 (1991) 3556.
[12] A. Mechler et al., Appl. Surf. Sci. 154 (2000) 22.
[13] F. Claeyssens et al., J. Appl. Phys. 89 (2001) 697.
[14] R.J. Lade, M.N.R. Ashfold, Surf. Coat. Tech. 120–121 (1999) 313.